

# Evaluation of Gamma Titanium Aluminide Matrix Composites as Potential Advanced Structural Materials for Future Space Transportation

Jason S. Craft<sup>1</sup>, Carrell E. Weeks<sup>1</sup> and W. Steven Johnson<sup>1,2</sup>

<sup>1</sup> George W. Woodruff School of Mechanical Engineering

<sup>2</sup> School of Materials Science Engineering

Georgia Institute of Technology

Atlanta, GA 30332, USA

## ABSTRACT

Very light-weight structures are necessary to meet the goals of advanced aerospace programs. Titanium matrix composites have been extensively evaluated for their potential to replace conventional superalloys in high temperature structural applications, with comparable mechanical performance and significant weight-savings. New gamma titanium aluminide alloys and a higher strain-to-failure silicon carbide fiber offer an improved TMC for use in intermediate temperature applications (400-800°C). The purpose of this investigation is aimed at evaluating the potential of a gamma titanium aluminide alloy with nominal composition Ti-46.5Al-4(Cr,Nb,Ta,B)at.% as a structural material in future aerospace transportation systems.

Monotonic tests were performed on fiber-less composite laminates to evaluate basic mechanical properties and stress-strain behavior of the gamma titanium alloy. Analytical predictions were made of the composite stress-strain response using AGLPLY.  $[0]_4$  composite lay-up was modeled to evaluate residual stresses after consolidation and the potential of these composites as structural materials. The analysis considered varying fiber volume ratios and two potential reinforcing fibers (Ultra-SCS and Nextel 610). High residual stresses were observed due to the CTE mismatch in the materials. For both composite systems, low fiber volume ratios were found necessary to prevent cracking of the composite during consolidation. Laminates with Nextel 610 fibers were found to offer potential for the stronger composite in this comparison.

## 1. INTRODUCTION

Metallic thermal protection systems are being evaluated for application in future reusable launch vehicles for increased durability and cost reductions associated with installation and routine maintenance. Current material systems under consideration include nickel superalloys, nickel aluminides, iron aluminides, and titanium aluminides. Titanium aluminide composites offer comparable mechanical performance characteristics with a significant weight-savings (30-50%) versus traditional nickel superalloys, for intermediate temperature applications (400°-800°C).

The objective of this research is to evaluate an advanced titanium aluminide alloy as a potential matrix material for structural aerospace applications. An analytical method is used to predict the fiber/matrix stress-strain response from fabrication and subsequent loading trials.

## 2. MATERIALS AND PROCEDURES

### 2.1. Analytical Method

AGLPLY is a 2-D laminate code that predicts composite response based on the properties of the constituents. Running from a DOS prompt, the program can operate on a 386 with Windows operating system. The program employs the vanishing fiber diameter (VFD) model, first proposed by Dvorak and Bahei-El-Din<sup>1</sup>. The vanishing fiber diameter model assumes the cylindrical fibers have a vanishing diameter, yet occupy a finite volume in the composite. The fibers contribute to the longitudinal stress state but do not interfere with the transverse deformation of the matrix. The assumption creates a uniform stress state in the transverse plane, effectively modeling the orthotropic symmetry of the composite. With a single-constraint condition in the axial direction, the governing equations are simplified, such that complex numerical analysis is not required.

Inputs to AGLPLY can be entered as lamina properties or fiber and matrix properties. These properties include Young's modulus, Poisson's ratio, coefficients of thermal expansion (CTE), yield stress, and stress-plastic strain curves. Each material property can be specified as a piece-wise function of temperature. Property data is linearly interpolated between specified points. The program only models elastic behavior if lamina properties are specified.

Loads that can be simulated include in-plane stress, out-of-plane normal stress, and uniform temperature change. The program has restart capabilities, allowing for input of piece-wise linear load-time functions in sequential jobs. This option allows for simulation of fabrication and experiments in sequential job steps. Spectrum load conditions can be applied as well. The program is capable of simulating load-control and strain-control conditions.

## 2.2. Fiber characterization

Two types of fibers were considered in the analysis: Specialty Material's Ultra-SCS silicon carbide fiber and 3M's Nextel 610 alumina fiber. The Ultra-SCS fiber is desirable because of its high stiffness and high tensile strength, but a significant thermal mismatch may cause problems with gamma titanium aluminide alloys. The Nextel 610 fiber, though less stiff and with a much lower tensile strength, has a higher CTE. Experimentally obtained mechanical properties were not available. Analysis relied on previously published data available in the literature and from the manufacturers.

Room temperature modulus was obtained for the Ultra-SCS fiber from Specialty Materials. Temperature dependent property data is readily available for the SCS-6 fiber<sup>3</sup> (also from Specialty Materials). As the composition of the two fibers is very similar, the assumption is made that temperature dependent trends would correlate between the SCS-6 and the Ultra-SCS fiber. A summary of representative material property data used for the Ultra-SCS silicon carbide fiber is provided in Table 1.

**Table 1** Ultra-SCS material parameters used in AGLPLY simulations<sup>7,8</sup>

Temperature, °C	Young's Modulus, GPa	Poisson's Ratio, $\nu$	CTE, mm/mm/°C
21	415	0.25	3.56E-06
315	403	0.25	3.73E-06
537	395	0.25	4.07E-06
871	381	0.25	4.57E-06

Room temperature Young's Modulus and CTE property data for the Nextel 610 fiber was obtained from 3M Corporation<sup>9</sup>. An estimate for Poisson's ratio was used for Al<sub>2</sub>O<sub>3</sub><sup>10</sup>. Since, temperature dependent property data was unavailable, mechanical properties were assumed to be independent of temperature for the Nextel 610 fiber. A summary of representative material property data used for the Nextel 610 alumina fiber is provided in Table 4.

**Table 2** Nextel 610 material parameters used in AGLPLY simulations<sup>9,10</sup>

Young's Modulus, GPa	Poisson's Ratio, $\nu$	CTE, mm/mm/°C
372	0.26	8.00E-06

## 2.3. Matrix Material

The material used in this study is  $\gamma$ -MET, produced by Plansee in Austria using their patented Advanced Sheet Rolling Process (ASRP)<sup>4</sup>. The nominal composition of the alloy is Ti-46.5Al-4(Cr,Nb,Ta,B)at.%, however the specific alloy content is proprietary to Plansee. The alloy is processed by ingot casting metallurgy and final consolidation by hot-isostatic pressing at nominal conditions of 1000°C, 18-ksi pressure, over a period of two hours<sup>5</sup>. Subsequent hot-rolling processes are employed to manufacture thin sheet product as small as 1mm thick.

In addition, gas-atomized alloy powder of the same composition was used for composite fabrication. The powder was low-pressure plasma-sprayed onto a rotating mandrel to produce thin foil. Layers of plasma-sprayed foil were stacked and consolidated using vacuum hot pressing to fabricate “fiber-less” composite panels to allow the assessment of the matrix properties.

#### *2.4. Experimental Procedures*

Monotonic tensile tests were conducted both on specimens of the rolled sheet material as well as specimens of the “fiber-less” composite panels to obtain general stress-strain behavior of the material. Dogbone coupons were cut from the panels by a WEDM process, having an overall length of 12.38cm, gage section of 5.78 cm, grip width of 1.52cm, reduced width of 1.02 cm, and a radius of curvature of 1.25cm.

The mechanical test setup consisted of a 22-kip servohydraulic test frame with water-cooled hydraulic grips and Teststar IIS computer control and data acquisition. Axial strain was measured with a high temperature extensometer with ceramic rods. The extensometer measured strain over a gage length of 2.5 cm and was capable of measuring strains up to 0.1 mm/mm. A 0°/90° strain gauge rosette was used under cyclic tension to measure Poisson effect in the material at room temperature.

A 2.5kW induction generator equipped with temperature controller, was used to heat the test specimen. The induction coil was fabricated in-house and was designed to maintain the temperature gradient to within  $\pm 10^\circ\text{C}$  of the desired temperature. A K-type thermocouple was spot-welded onto the gage section of the test specimen to monitor the temperature.

Dilatometry was used to collect thermal expansion data. The dilatometer utilized a Thermal Technology Model 1000-2560-FP furnace comprised of a water-cooled housing with graphite heating elements and fibrous insulation, for which inert and reducing environments were appropriate. In conjunction with the furnace, a differential graphite dilatometer was used to measure specimen displacement via a linear variable differential transformer (LVDT).

### **3. RESULTS & DISCUSSION**

#### *3.1. Experimental Matrix Characterization*

Monotonic tensile tests were conducted using coupons of the  $\gamma$ -MET sheet material to obtain the general stress-strain behavior of the material. The tests were conducted under isothermal conditions at 21°C and 650°C respectively, in strain control. In addition, two sets of mechanical tests were performed on the fiber-less composite specimens. Strain-controlled testing was conducted to determine the equilibrium stress-strain response, and load-controlled testing was conducted to determine the rate-dependent deformation. Tests were conducted at 21°C and 450°C. The fiber-less composite specimens exhibited brittle failure prior to yielding and thus valid values of yield strength, tensile strength, and total strain were not obtained. Measurements of the modulus for both the sheet material and the fiber-less

composite material were close to other published results in the literature (see Figure 1), though the ductility is significantly less.

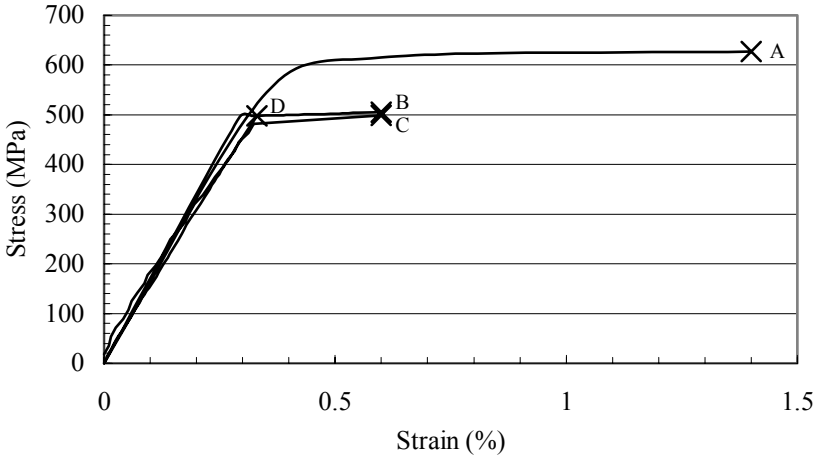


**Figure 1** Room temperature material property data for A) optimal properties found in the literature, B) NASA LaRC testing of consolidated fiber-less composite, C) rolled sheet material specimens, and D) consolidated fiber-less composite specimens

Visual inspection indicated good consolidation of the fiber-less composites, but inhomogeneities were observed in the cross-section from scanning electron microscopy examination (see Figure 2). The dark regions were presumed to be large gamma grains. Bulk chemical analysis indicated no significant contamination during consolidation, but a thin Mo-rich surface layer was observed which could have contributed to the low ductility.

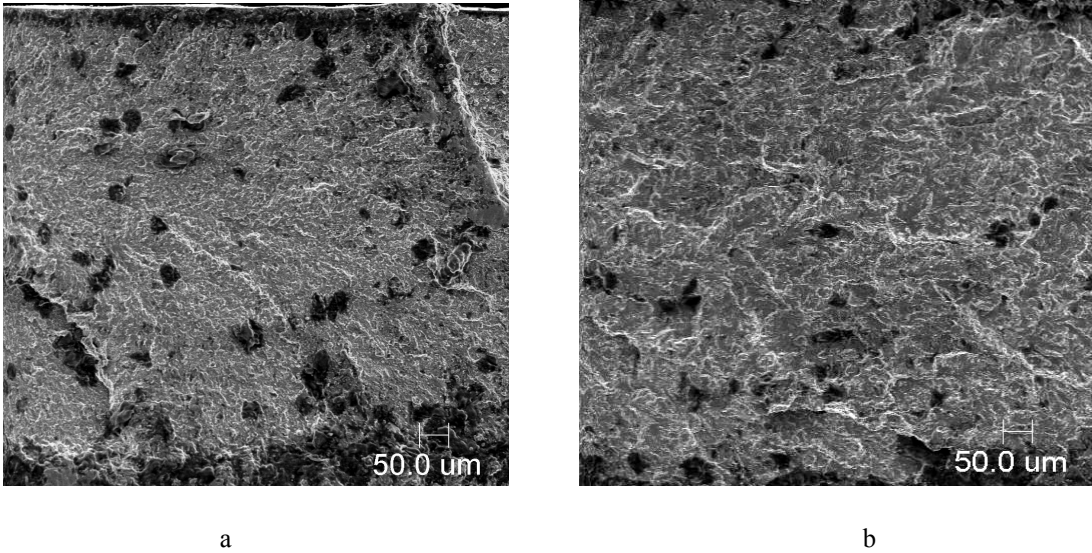


**Figure 2** Fracture surfaces of a) fiber-less composite and b) monolithic sheet tensile specimens tested at 21°C

Inputs for AGLPLY include coefficient of thermal expansion, Poisson’s ratio, Young’s modulus, yield strength, and stress-plastic strain curves as a function of temperature. The thermal expansion in the rolling direction of the sheet material was measured from the results of a dilatometer experiment. The coefficients of thermal expansion from room temperature up to 850 °C are plotted in Figure 3.

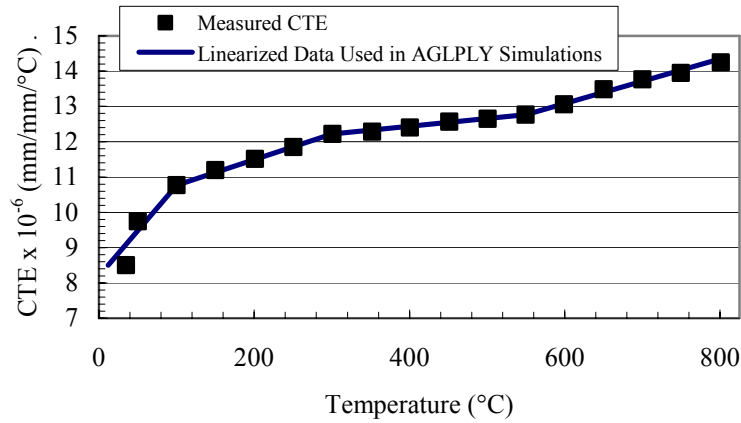


**Figure 3** Coefficient of thermal expansion of  $\gamma$ -MET monolithic sheet as function of temperature

Tensile data published in Clemens et al.<sup>4</sup> was used to approximate the Young's modulus, yield strength, and stress-plastic strain behavior for this analysis. Stress-strain curves were approximated using the published yield strength, ultimate tensile strength and failure strain data. The Poisson ratio was measured using a  $0^\circ/90^\circ$  strain gage rosette under tensile cyclic loading. The material inputs for AGLPLY are given in Table 1.

**Table 3**  $\gamma$ -MET material parameters used in AGLPLY simulations

Temperature, °C	Elastic Modulus <sup>4</sup> , GPa	Poisson's Ratio, $\nu$	CTE, mm/mm/°C	Yield Stress <sup>4</sup> , MPa	Plastic Stress-Strain Curve <sup>4</sup> , MPa		Ultimate Tensile Strength <sup>4</sup> , MPa	Total Elongation <sup>4</sup> , %
					(0.6% Elong.)	(1.2% Elong.)		
21	155	0.244	8.50E-06	545	588	616	627	1.4
100	153	0.244	10.77E-06	527	580	610	615	1.6
300	149	0.244	12.22E-06	498	566	583	595	2.1
550	140	0.244	12.77E-06	475	530	550	672	5.0
700	135	0.244	13.76E-06	471	510	518	668	21.9
800	127	0.244	14.35E-06	380	399	400.6	437	69

### 3.2. Analytical Modeling of Composite Behavior During Consolidation

The first step was to analyze the residual stresses that developed as a result of thermal mismatch during consolidation. The constituents are consolidated at high temperatures and then the materials are allowed to cool in the furnace to room temperature. The CTE of the matrix is larger than the fiber, so tensile residual stresses develop in the matrix upon cooling. If the stresses in the matrix exceed the material's tensile strength, cracking and damage will result. Due to the brittle nature of the alloy, extensive cracking has been observed in recent consolidation trials of a  $[0]_4$  SCS-6/ $\gamma$ -MET laminate at NASA LaRC (see Figure 4).

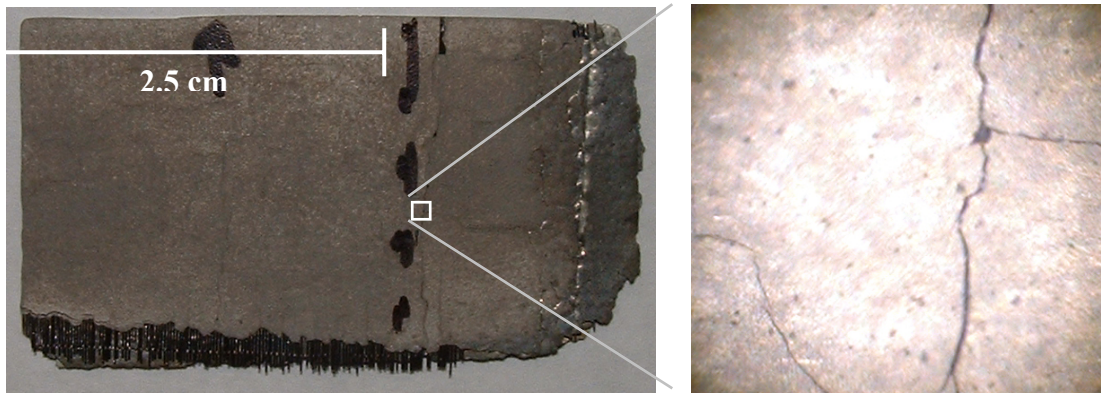


**Figure 4** Cracking in  $[0]_4$  SCS-6/ $\gamma$ -MET after consolidation

For this purpose, cooling from consolidation temperature was simulated for a  $[0]_4$  laminate to calculate the residual stresses that develop in the constituents. It is not known at what temperature the fiber and matrix “lock-up” during cooling from consolidation. For other TMCs, generally, it has been assumed that creep relieves any thermal stresses that develop at temperatures greater than one half of the melting point of the matrix<sup>3</sup>. For the AGLPLY analysis, a “lock-up” temperature of 725°C was initially assumed, corresponding to half the melting point of the  $\gamma$ -MET alloy ( $\sim 1450^\circ\text{C}^{11}$ ). However, in the recent consolidation trials of a  $[0]_4$  SCS-6/ $\gamma$ -MET laminate at NASA LaRC, transverse cracking due to thermal mismatch was observed for fiber volume fractions as low as 20%, implying a higher “lock-up” temperature than initially assumed. Based on these observations and the tensile data for the fiber-less composite, which demonstrated an ultimate stress at 497 MPa, a “lock-up” temperature of 925°C was determined using AGLPLY analysis.

As could be seen in Figure 1, the consolidated samples resulting from the recent trials at NASA LaRC do not possess the optimal properties that have been seen in this alloy. Therefore an analysis using the lock-up temperature determined by the recent consolidation trials and the higher properties seen in the literature for the alloy were used to determine the feasibility of manufacturing a SCS-6/ $\gamma$ -MET laminate assuming that optimal matrix properties could be achieved. Residual axial stresses of the matrix for varying fiber volumes for an  $[0]_4$  Ultra-SCS/ $\gamma$ -MET composite are shown in Figure 5.

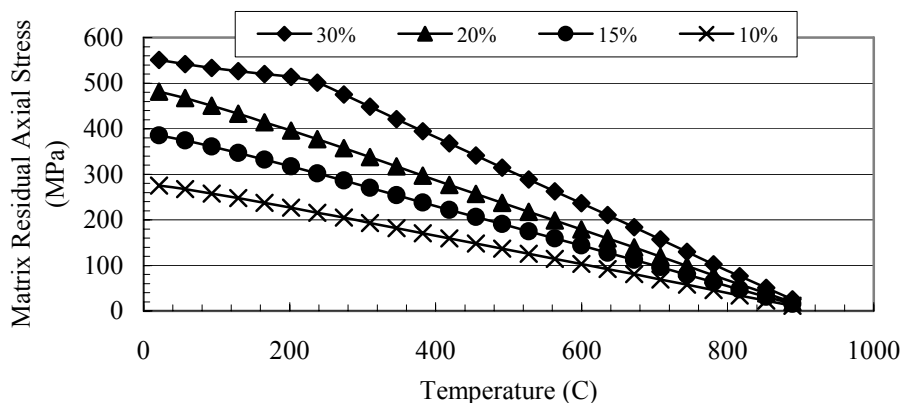


**Figure 5** Matrix residual axial stress due to thermal mismatch for varying fiber volumes of an  $[0]_4$  Ultra-SCS/ $\gamma$ -MET composite

The residual axial stress that develops in the matrix is high, with yielding predicted at about 225°C during cool-down for a composite with 30%  $V_f$ . While AGLPLY does not predict matrix yielding upon cool-down with a volume fraction of 20%, the usefulness of the

laminate is unclear when considering the amount of additional load that can be applied in service before eventual yielding occurs in the matrix.

The residual axial stress of the matrix modeled with varying volume fractions of Nextel 610 fibers is shown in Figure 6. Similar trends were observed in this laminate, when comparing it with the  $[0]_4$  Ultra-SCS/ $\gamma$ -MET composite. The overall magnitude of residual stresses was lower than the previous analysis, attributed to the higher CTE of the Nextel 610 alumina fiber.

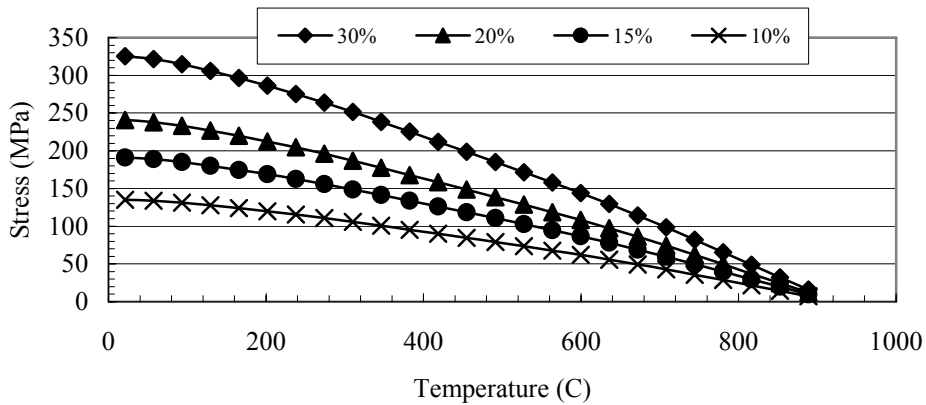


**Figure 6** Matrix residual axial stress due to thermal mismatch for varying fiber volumes of an  $[0]_4$  Nextel 610/ $\gamma$ -MET composite

The generic flight profile previously generated for TMCs in the NASP program<sup>3</sup> was used as a guideline in evaluating the monotonic response of these laminates. Tensile stress-strain curves were generated for the laminates at 21°C, 400°C, and 650°C under isothermal conditions and monotonic loading to a laminate stress of 300 MPa, applying matrix yielding as a failure criterion.

Table 4 lists stiffness and maximum laminate stress (based on pure elastic behavior in the constituents) for Ultra-SCS/ $\gamma$ -MET laminates with varying fiber volume ratios. With a composite strength (based on matrix yield criteria) of 315 MPa and an effective Young's Modulus of 181 GPa, a fiber volume fraction of 10% was close to a maximum reinforcement without sacrificing the usefulness of the laminate.

**Table 4** Overall laminate properties of  $[0]_4$  Ultra-SCS/ $\gamma$ -MET at 21°C

Fiber Content	Young's Modulus, GPa	Load Capacity (No Yielding), MPa
30%	129	0
20%	207	74
15%	194	200
10%	181	315
0%	155	545

The trends in stress-strain behavior of the Nextel 610/ $\gamma$ -MET laminates were similar to laminates with silicon carbide reinforcement. One difference to note is a lower stiffness for equal fiber content because of the lower modulus of the alumina fiber. However, with lower residual stresses, larger fiber content can be used, and the laminate can withstand higher loads. Table 5 lists stiffness and maximum laminate stress (based on pure elastic behavior in the constituents) for laminates with varying fiber volume ratios. With a composite strength of

389 MPa and a modulus of 204 GPa, a fiber volume fraction of up to 20% could be achieved without sacrificing the usefulness of the laminate.

**Table 5** Overall laminate properties of  $[0]_4$  Nextel 610/ $\gamma$ -MET at 21°C

Fiber Content	Young's Modulus, GPa	Load Capacity (No Yielding), MPa
30%	214	312
20%	204	389
15%	194	428
10%	184	582
0%	155	545

As temperature increases, the toughness of the alloy increases while the matrix residual stresses decrease, along with the stiffness. The overall effect was the laminate could carry more load, and thus these materials show great promise for elevated temperature application. However, it is important to note that even though the structures heat up during flight, significant loads would be applied at lower temperatures, during take-off and initial flight maneuvers. Therefore, focus on room temperature performance is critical.

#### 4. CONCLUSIONS

Monotonic testing was conducted on samples of the fiber-less composite form of the alloy as well as rolled sheet specimens to experimentally determine the stress-strain response for use in analysis. Modeling was conducted to evaluate composite consolidation and the resulting thermal mismatch and potential mechanical behavior of  $[0]_4$  laminates with a  $\gamma$ -MET matrix. Silicon carbide (Ultra-SCS) and alumina (Nextel 610) fibers were selected as reinforcing materials. From the analysis, the following were significant findings:

- The CTE of the  $\gamma$ -MET alloy ( $8.50E-6$  /°C) was significantly higher than the Ultra-SCS silicon carbide fiber ( $3.56E-6$  /°C), such that thermal mismatch would be a problem in composites.
- Modeling of consolidation trials with a 30% fiber content predicted in high residual stresses matrix yielding in the Ultra-SCS/ $\gamma$ -MET laminate and high residual stress in the Nextel 610/ $\gamma$ -MET laminate.
- With a higher CTE, the Nextel 610 is a closer thermal match with the  $\gamma$ -MET alloy, and lower residual stresses develop as a result.
- For laminates with Ultra-SCS reinforcement, it was predicted that a maximum of ~10% fiber content could be added, resulting in a laminate with an elastic modulus of 181 GPa and a maximum load capacity of 315 MPa without yielding in the matrix.
- For laminates with Nextel 610 reinforcement, it was predicted that up to a ~20% fiber content could be added, resulting in an effective modulus of 204 GPa and a maximum load capacity of 389 MPa without yielding in the matrix.
- From this analysis, it appears that Nextel 610/ $\gamma$ -MET offers the potential for a stronger composite system.
- Observations of foil fabrication and consolidation indicate that this process must be optimized to achieve better room temperature ductility in order to successfully manufacture  $\gamma$ -MET matrix composites.

## ACKNOWLEDGEMENTS

The previous research was sponsored by NASA Langley Research Center, Grant #NAG-1-02018. Technical monitor for the program was Keith Bird. The authors would also like to thank Dr. Robert Speyer for providing dilatometry equipment for thermal expansion testing.

## References

1. **Dvorak, G. J.** and **Bahei-El-Din, Y. A.**, “Plasticity Analysis of Fibrous Composites”, *Journal of Applied Mechanics*, **49** (1982), 327-335.
2. **Eisenberg, M.A.**, and **Yen, C.-F.**, “A Theory of Multiaxial Anisotropic Viscoplasticity”, *ASME Journal of Applied Mechanics*, **48** (1981), 276-284.
3. **Mirdamadi, M.**, and **Johnson, W.S.**, “Prediction of Stress-Strain Response of SCS-6/Timetal-21S subjected to a hypersonic flight profile”, *Composites Part A*, **27A** (1996), 1033-1040.
4. **Clemens, H.**, **Kestler, H.**, **Eberhardt, N.**, and **Knabl, W.**, “Processing of  $\gamma$ -TiAl Based Alloys on an Industrial Scale”, *Gamma Titanium Aluminides*, TMS, Warrendale, PA (1999), 209-223.
5. **Leholm, R.**, **Norris, B.**, and **Gurney, A.**, “High Temperature Alloys for Aerospace Structures”, *Advanced Materials and Processes*, **159/5** (2001), 27-31.
6. ASTM E8-01, “Standard Test Methods for Tension Testing of Metallic Materials”, reprinted from *Annual Book of ASTM Standards*, American Society for Testing and Materials, West Conshohocken, PA, 1999.
7. **Pollock, W.D.**, and **Johnson, W.S.**, “Characterization of Unnotched SCS-6/Ti-15-3 Metal Matrix Composites at 650°C”, *Composite Materials: Testing and Design (Tenth Volume)*, ASTM STP 1120 (1992), 175-191. **Askeland, D.R.**, *The Science and Engineering of Materials*, 3<sup>rd</sup> Ed., PWS Publishing Co., Boston, MA, 1994, pp. 743-6.
8. **Smith, P.R.** and **Rosenberger, A. H.**, “Orthorhombic Titanium Aluminide Metal Matrix Composites (O TMCs) – A Review”, Report # AFRL-ML-WP-TR-2000-4083.
9. **Kim, Y.-W.**, “Intermetallic Alloys Based on Gamma Titanium Aluminide”, *JOM*, vol. 41, no. 7, 1989, pp. 24-30. <http://www.3m.com/market/industrial/mmc/nextel.html>
10. <http://www.3m.com/market/industrial/mmc/nextel.html>
11. **Askeland, D.R.**, *The Science and Engineering of Materials*, 3<sup>rd</sup> Ed., PWS Publishing Co., Boston, MA, 1994, 743-6.
12. **Kim, Y.-W.**, “Intermetallic Alloys Based on Gamma Titanium Aluminide”, *JOM*, **41/7** (1989), 24-30.